Physics of organic-organic interfaces

Jarzab, Dorota Maria

Chapter 7

Charge Separation Dynamics in Inorganic-Organic Ternary Blend for Efficient Infrared Photodiodes

In this Chapter, we investigate the working mechanism of the hybrid ternary blend, composed of PbS-NCs, poly(3-hexylthiophene) (P3HT) and the fullerene derivatives [6,6]-phenyl-C61-butyric acid methyl ester (PCBM). To understand the role of each component in the heterojunction we studied the photoluminescence dynamics of the binary and ternary hybrid thin films both in the visible and near-infrared spectra range.[*]

[*] D. Jarzab, K. Szendrei, M. Yarema, S. ten Cate, J. Schins, L. D. A. Siebbeles, W. Heiss, M. A. Loi, *Submitted*, 2010.

7.1 Introduction

Solution-processed inorganic-organic hybrid devices are one of the most promising low-cost alternatives to epitaxially grown, inorganic electronics. In these hybrid devices the active layer is composed of a mixture of inorganic and organic semiconductors that are often blends of colloidal inorganic nanocrystals (NCs) and organic molecules.[1-4]

In the hybrid heterojunctions generally the NCs are working as sentitizers while the organic serves as functional interface to extract carriers or energy from the nanocrystals.[1],[2] Although the fabrication of this kind of heterostructures resulted to be rather challenging, several groups have reported in the last years the successful application of binary inorganic-organic heterojunctions consisting of NCs and organic semiconductors for light emitting diodes,[3],[5] solar cells[4], and near-infrared (NIR) photodetectors.[1],[6],[7] More recently, ternary blends composed of inorganic NCs and two organic materials have attracted the researchers' attention.[8-11]

T. Rauch et. al.[2] have reported for the first time solution-processed, high performing, inorganic-organic hybrid photodiodes for infrared imaging. These photodiodes, composed by a combination of NIR sensitive NCs (PbS) with polymer/fullerene blend, show a responsivity[c] of 0.5 AW^{-1} and detectivity[d] of 2.3×10^9 Jones. Although the authors propose an explanation of the working mechanism of the photodiodes based on energy level alignment of the component materials, experiments thoroughly elucidating the working mechanism and the interaction between the NCs and the organic materials have not yet been performed. Any further development of hybrid devices requires an understanding of processes such as charge separation and charge transfer between the inorganic and organic components.

In this study, we investigated the working mechanism of the hybrid ternary blend, composed of PbS-NCs, poly(3-hexylthiophene) (P3HT) and the fullerene derivatives [6,6]-phenyl-C61-butyric acid methyl ester (PCBM). As previously mentioned this hybrid has shown excellent performance when used as active layer in NIR photodiodes.[2] To understand the role of each component in the heterojunction we studied the photoluminescence dynamics of the binary and ternary hybrid thin films both in the visible and near-infrared spectra range.

[c] Responsivity measures the input–output gain of a detector system.
[d] Detectivity is the normalized radiation power required to give a signal from a photoconductor that is equal to the noise.

In the ternary blend we observed a reduction of the PL intensity and decay time both in the visible and near-infrared spectral range. In the visible, this is attributed to the electron transfer from P3HT to PbS and PCBM. While in the NIR it is ascribed to the electron transfer from PbS towards PCBM and to the hole transfer towards P3HT.

Noticeably, when monitoring the near-infrared emission the charge transfer is enhanced in the ternary blend with respect to the binary blend.[1] This is due to the concomitant hole transfer occurring between the PbS-NCs and the P3HT that has the effect to deplete the long lived holes' population established after the electron transfer, boosting the efficiency of the excitonic splitting. THz-TDS results confirm the negligible mobility of the binary PbS:P3HT blend while mobile carriers in the ternary PbS:P3HT:PCBM have a lifetime exceeding 10 ns.

7.2 Results and discussion

Figure 7.1 shows the chemical structure and the schematic energy level diagrams of P3HT, PbS-NCs and PCBM. PbS-NCs are semiconducting particles showing NIR sensitivity, with the absorption edge tunable between 800–1800 nm. The P3HT:PCBM blend is a well known active medium for organic solar cells.[12],[13] The blend shows good hole and electron mobility,[14],[15] however, this organic blend absorbs only up to 650 nm.[16] The incorporation of PbS-NCs into P3HT:PCBM heterojunctions results in an expansion of the absorption down to the near-infrared with an edge that depends upon the NCs size, with preservation of ambipolar transport.

The schematic energy level diagram of the ternary blend (Figure 7.1) suggests that different processes can occur depending on the excitation energy. When excitons are formed upon light absorption in the PbS-NCs, it is expected that the electrons will be transferred to PCBM and holes to P3HT. When excitations are generated in P3HT, we can predict from the energy levels that an electron transfer will occur towards PbS and/or PCBM. However, the energy levels reported in Figure 7.1 are rough estimations (in particular in the case of the NCs[17]), and the picture previously described, although possible, has not been demonstrated. To learn more about the processes occurring between the blend components, we investigated steady state and time-resolved PL.

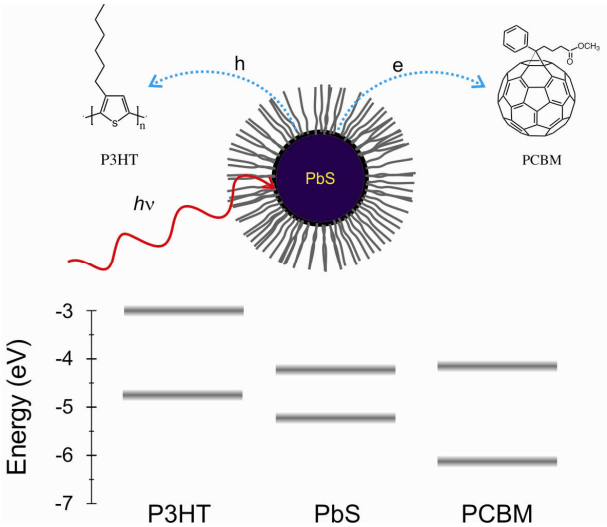

Figure 7.1. Chemical structure of P3HT, PCBM and cartoon of the PbS-NCs with ligands; lower part: schematic energy level diagram of P3HT, PCBM and of PbS-NCs.

Figure 7.2(a) shows the normalized VIS PL emission of the drop-casted thin films of neat P3HT, PbS:P3HT, P3HT:PCBM, and PbS:P3HT:PCBM blends. All blends display similar features deriving from P3HT. The PL emission is characterized by two vibronic peaks centered at ~675 nm and at ~707 nm with a shoulder at ~805 nm. Only the PL emission of neat P3HT film shows slightly different spectral shape, with partial reduction of the 0-0 vibronic transition, most likely because of the self absorption of the emitted light due to the large layer thickness of P3HT thin film layer.[18] The PL emission of all 3 blends shows no significant changes in the spectral shape and peak energy, but does show a substantial difference in the overall photoluminescence intensity. In particular, the ternary blend PL displays a pronounced quenching with respect to the photoluminescence of the neat polymer and the PbS:P3HT blend. However, due to the different thickness of the film it is not possible to directly compare the PL intensities.

Figure 7.2(b) shows the dynamics of the PL of P3HT, PbS:P3HT, P3HT:PCBM and PbS:P3HT:PCBM thin films. The PL decays were detected at ~675 nm that correspond to the 0-0 vibronic transition of P3HT. All samples show a bi-exponential decay. The neat P3HT film displays the slowest decay, fitted with time constants $\tau_1 \approx 40$ ps and $\tau_2 \approx 488$ ps. The blend composed by P3HT and NCs shows a reduction of the long time constant of ~132 ps, i.e., and the PL decay can be fitted with $\tau_1 \approx 40$ ps and $\tau_2 \approx 356$ ps. The reduced PL decay time in the PbS:P3HT blend indicates the occurrence of a charge transfer from the excited P3HT to the NCs, which is most probably an electron transfer (see Figure 7.1).

In the case of the ternary blend, the decrease of PL life time is even more pronounced; the PL decay of the PbS:P3HT:PCBM thin film can be modelled using $\tau_1 \approx 8$ ps and $\tau_2 \approx 36$ ps. These time constants are comparable to the values obtained for the P3HT:PCBM thin film indicating a similar electron transfer efficiency.

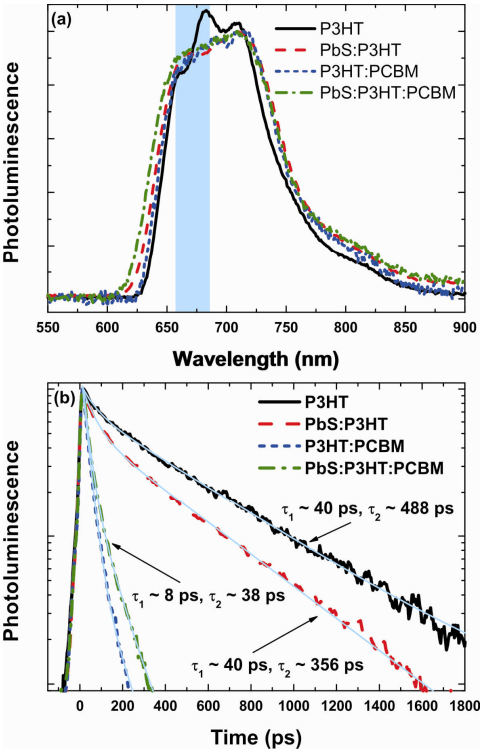

Figure 7.2. VIS Photoluminescence spectra (a) and dynamics detected at ~ 675 nm (b) of P3HT, PbS:P3HT, P3HT:PCBM and PbS:P3HT:PCBM drop-casted films.

Figure 7.3(a) shows the normalized NIR PL spectra of the drop-casted films of PbS-NCs, PbS:P3HT, PbS:PCBM, and PbS:P3HT:PCBM. The PL emission of PbS-NCs is characterized by a Gaussian-shaped band, centred at ~1006 nm with the full width at half maximum (FWHM) of ~100 nm. The PL spectra of the PbS:P3HT blend is blue shifted of ~23 nm with respect to the PbS thin film. It can be also described by a Gaussian function with maximum at ~983 nm and FWHM of ~124 nm. The normalized PL spectra of the PbS:PCBM and PbS:P3HT:PCBM blends overlap completely. As previously, in this case, the PL band can be described by a Gaussian function blue shifted with respect to the neat PbS crystals of ~70 nm. The spectrum of this blend as the one of PbS:P3HT, shows a shoulder

at ~860 nm originating from the tail of the emission of P3HT and/or PCBM not cut by the low pass filter. The large blue shift observed in the blends, compared to the

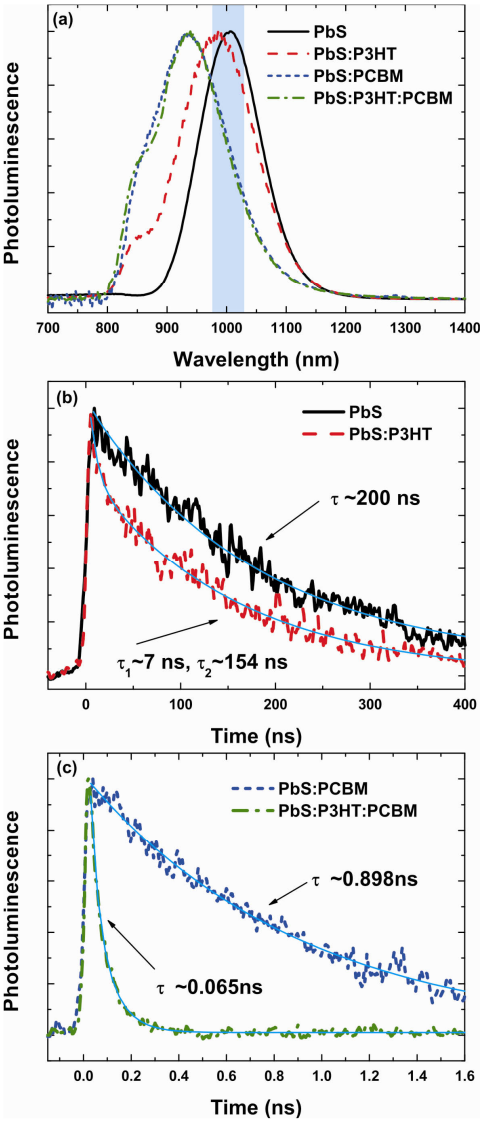

Figure 7.3. NIR photoluminescence spectra (a) and dynamics detected at ~ 1006 nm of PbS, PbS:P3HT (b) and PbS:PCBM, PbS:P3HT:PCBM (c) drop-casted films. The blue band in panel (a) indicates the wavelengths over which the dynamic traces are integrated

pristine NCs films, can be ascribed both to the variation of the dielectric constant of the medium (ε of PCBM is ~3.9[14], of P3HT is ~3[19], while for PbS is ~17[20]) and also to the charge transfer that results in the emission from higher lying electronic states. Taking into account the different shift detected for the PbS:P3HT

blend with respect to the ternary blend, we can infer a less effective charge transfer for the first sample.

The NIR PL dynamics of PbS-NCs, PbS:P3HT and PbS:PCBM, PbS:P3HT:PCBM thin films are reported in Figure 7.3(b) and (c), respectively. The PL decays were detected at ~1006 nm, corresponding to the maximum PL intensity of neat PbS-NCs film, and no considerable difference was detected at other wavelengths. The PL of the PbS-NCs thin film has mono-exponential decay with time constant of ~200 ns, by blending the NCs with P3HT we observe a bi-exponential lifetime with the first decay constant $\tau_1 \approx 7$ ns and the second $\tau_2 \approx 154$ ns. The amplitude of these two time components shows wavelength dependence: at shorter wavelength the fast component is more pronounced, while at longer wavelength the slow component is dominant. Despite the observed decrease of the decay time, which can be interpreted as due to the hole transfer from excited PbS-NCs to P3HT, the magnitude of the reduction (200 ns → 154 ns) shows the low efficiency of the process. The low efficiency of the charge transfer between PbS-NCs and P3HT is also reflected in the poor external quantum efficiency (EQE≈0.2%) of the photodiode using the same binary blend as active layer.

In Figure 7.3(c) the PL dynamics of the PbS:PCBM and PbS:P3HT:PCBM films are reported. The NCs PL emission in the PbS:PCBM film is reduced from hundreds of nanoseconds to hundreds of picoseconds, the decay is mono-exponential with time constant $\tau \approx 898$ ps. This is the signature of the efficient, ultrafast electron transfer from the NCs to the fullerene molecules that we have previously reported.

Noteworthy, in the ternary blend we observed a further reduction of the dynamics of the NCs emission with a lifetime of $\tau \approx 65$ ps. This is more than one order of magnitude faster than that of the PbS:PCBM blend and four orders of magnitude faster than that of the neat PbS-NCs film. The schematic summary of the excitation and charge transfer pathways as obtained from the time-resolved measurements is depicted in Figure 7.4. To estimate the efficiency of the charge transfer processes we calculated its rate: $k = (1/\tau_{BH} - 1/\tau_{ref})$, where τ_{BH}, τ_{ref} are the PL decay times of the blend and of the reference neat sample, respectively. Figure 7.4(a) and (b) illustrate the possible excitations for the binary blend both with excitation in the visible (P3HT) and in the infrared (NCs); the transfer rate of each process is indicated. Figure 7.4(c) reports excitation processes and transfer rates for the ternary blends.

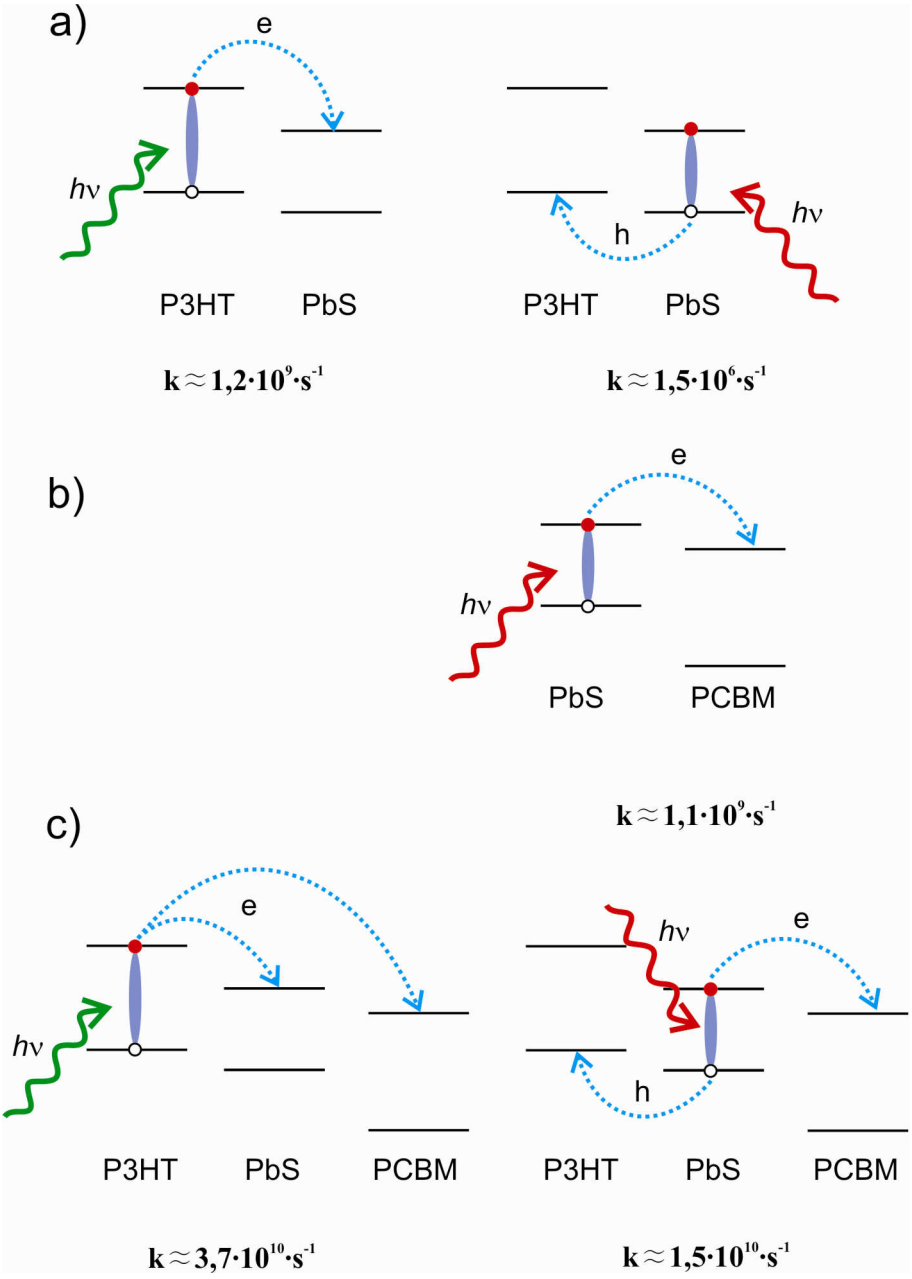

Figure 7.4. Schematic of the excitation and charge transfer pathways in: (a) PbS:P3HT blend, (b) PbS:PCBM blend; (c) PbS:P3HT:PCBM blend. For Figure 4c the transfer rates take in account the sum of the processes indicated with the arrow

The elevate transfer rate $1{,}5 \cdot 10^{10} \cdot s^{-1}$ of the ternary blend correlates with the high efficiency of the photodiodes made with this active layer.[2] This is why the

understanding of the excitation dynamics of the ternary blend is extremely relevant. It is important to notice that the ternary blend shows an order of magnitude higher transfer rate respect to the blend composed by PbS and PCBM. This difference cannot be justified by the opening of a second transfer path towards P3HT, in fact this process can eventually account for a rate (1,5·106·s-1) that is 4 order of magnitude smaller that the one of the ternary blend. We have recently described how in the PbS:PCBM samples the holes remain trapped in the PbS NCs, after the electron transfer.[1] In the case of the ternary blend the hole population is not accumulated because holes can be effectively transferred to P3HT. We suggest that the depletion of the hole population in the NCs allows the efficient regeneration that are then available for separation. The presence of both P3HT and PCBM not only enables the ambipolar transport in devices but also facilitates the charge extraction from the PbS-NCs.

7.3 Conclusions

Insight into the working mechanism of hybrid blends used for efficient near-infrared photodiodes was obtained by time-resolved photoluminescence and terahertz photoconductivity studies. We compared the properties of the PL emission of the ternary PbS:P3HT:PCBM blend and the binary PbS:P3HT, PbS:PCBM and P3HT:PCBM blends with the PL of the pristine PbS-NCs and P3HT. In the ternary blend the efficiency of the charge transfer is significantly enhanced compared to the PbS:P3HT and PbS:PCBM blends, indicating that both hole and electron transfer from excited NCs to the polymer and fullerene occur, respectively. The hole transfer towards the P3HT determines the equilibration of their population in the NCs after the electron transfer towards PCBM, allowing their re-excitation and new charge transfer. The experimental results allow us to understand the role of each component in the ternary PbS:P3HT:PCBM blends.

7.4 Experimental details

Materials: Oleic-acid-capped PbS-NCs were synthesized as reported in ref.[21] We used PbS-NCs with diameters of 3.4 nm, showing absorption maximum at ~ 870 nm, with the highest occupied molecular orbital (HOMO) level of ~ -5.1 eV and the lowest unoccupied molecular orbital (LUMO) level of ~ -3.7 eV.
The fullerene derivative [6,6]-phenyl-C61-butyric acid methyl ester (PCBM) were obtained from Solenne Bv. P3HT with regioregularity of 98,5% was purchased from Rieke Metals.

Sample Fabrication: Thin films of PbS, P3HT, PbS:P3HT, PbS:PCBM, P3HT:PCBM, and PbS:P3HT:PCBM were drop-casted onto quartz substrate from 5mg/ml chlorobenzene solution. The solutions were prepared in nitrogen atmosphere. The weight ratio between the blended components were: 1:1 for PbS:P3HT; 1:1 for PbS:PCBM; 1:1 for P3HT:PCBM; and 1:1:1 for PbS:P3HT:PCBM. Prior to processing, the substrates were cleaned with a standard wet-cleaning procedure, combining ultrasonic cleaning in acetone and isopropanol.
Spectroscopy: The traces of the PL decay time were integrated in a spectral region of about 20 nm, at the 0-0 excitonic transition in the visible, and at ~1006 nm, (corresponding to the excitonic peak of neat PbS-NCs). All samples, both in the visible and in the NIR, showed no considerable difference at other wavelengths. Samples containing PbS were also excited at 760 nm showing no significant difference respect to the higher energy excitation.

All samples were measured in several locations; the variations in the results of the time-resolved PL measurements did not exceed the resolution of the instrument.

References

[1] K. Szendrei, F. Cordella, M. V. Kovalenko, M. Böberl, G. Hesser, M. Yarema, D. Jarzab, O. V. Mikhnenko, A. Gocalinska, M. Saba, et al., *Adv. Mater.* **2009**, *21*, 683-687.

[2] T. Rauch, M. Boberl, S. F. Tedde, J. Furst, M. V. Kovalenko, G. Hesser, U. Lemmer, W. Heiss, O. Hayden, *Nat Photon* **2009**, *3*, 332-336.

[3] N. Tessler, V. Medvedev, M. Kazes, S. Kan, U. Banin, *Science* **2002**, *295*, 1506-1508.

[4] W. U. Huynh, J. J. Dittmer, A. P. Alivisatos, *Science* **2002**, *295*, 2425-2427.

[5] B. O. Dabbousi, M. G. Bawendi, O. Onitsuka, M. F. Rubner, *Appl. Phys. Lett.* **1995**, *66*, 1316.

[6] S. A. McDonald, G. Konstantatos, S. Zhang, P. W. Cyr, E. J. D. Klem, L. Levina, E. H. Sargent, *Nat Mater* **2005**, *4*, 138-142.

[7] G. Konstantatos, I. Howard, A. Fischer, S. Hoogland, J. Clifford, E. Klem, L. Levina, E. H. Sargent, *Nature* **2006**, *442*, 180-183.

[8] M. Park, B. D. Chin, J. Yu, M. Chun, S. Han, *J. Ind. Eng. Chem.* **2008**, *14*, 382-386.

[9] A. J. Morfa, K. L. Rowlen, T. H. Reilly, M. J. Romero, J. van de Lagemaat, *Appl. Phys. Lett.* **2008**, *92*, 013504.

[10] B. V. K. Naidu, J. S. Park, S. C. Kim, S. Park, E. Lee, K. Yoon, S. Joon Lee, J. Wook Lee, Y. Gal, S. Jin, *Sol. Energy Mater. Sol. Cells* **2008**, *92*, 397-401.

[11] J. N. de Freitas, I. R. Grova, L. C. Akcelrud, E. Arici, N. S. Sariciftci, A. F. Nogueira, *J. Mater. Chem.* **2010**, DOI 10.1039/c0jm00191k.

[12] Y. Kim, S. Cook, S. M. Tuladhar, S. A. Choulis, J. Nelson, J. R. Durrant, D. D. C. Bradley, M. Giles, I. McCulloch, C. Ha, et al., *Nat Mater* **2006**, *5*, 197-203.

[13] J. Y. Kim, S. Kim, H. Lee, K. Lee, W. Ma, X. Gong, A. Heeger, *Adv. Mater.* **2006**, *18*, 572-576.

[14] V. Mihailetchi, J. V. Duren, P. Blom, J. Hummelen, R. Janssen, J. Kroon, M. Rispens, W. Verhees, M. Wienk, *Adv. Funct. Mater.* **2003**, *13*, 43-46.

[15] V. D. Mihailetchi, H. Xie, B. de Boer, L. M. Popescu, J. C. Hummelen, P. W. M. Blom, L. J. A. Koster, *Appl. Phys. Lett.* **2006**, *89*, 012107.

[16] D. Jarzab, F. Cordella, M. Lenes, F. B. Kooistra, P. W. M. Blom, J. C. Hummelen, M. A. Loi, *J. Phys. Chem. B* **2009**, *113*, 16513-16517.

[17] B. Hyun, Y. Zhong, A. C. Bartnik, L. Sun, H. D. Abruña, F. W. Wise, J. D. Goodreau, J. R. Matthews, T. M. Leslie, N. F. Borrelli, *ACS Nano* **2008**, *2*, 2206-2212.

[18] E. Tekin, H. Wijlaars, E. Holder, D. A. M. Egbe, U. S. Schubert, *J. Mater. Chem.* **2006**, *16*, 4294-4298.

[19] J. Szmytkowski, *Chem. Phys. Lett.* **2009**, *470*, 123-125.

[20] L. Cademartiri, J. Bertolotti, R. Sapienza, D. S. Wiersma, G. von Freymann, G. A. Ozin, *J. Phys. Chem. B* **2006**, *110*, 671-673.
[21] M. Hines, G. Scholes, *Adv. Mater.* **2003**, *15*, 1844-1849.